Available online at www.sciencedirect.com
ScienceDirect
Journal of Power Sources 158 (2006) 879–884
JOURNAL OF POWER SOURCES
www.elsevier.com/locate/jpowsour

Short communication

Lead-acid batteries with foam grids

S.M. Tabaatabaai [a], M.S. Rahmanifar [b,*], S.A. Mousavi [a], S. Shekofteh [a], Jh. Khonsari [a], A. Oweisi [a], M. Hejabi [a], H. Tabrizi [a], S. Shirzadi [a], B. Cheraghi [a]

[a] *R&D of Niru Battery Manufacturing Co. Pasdaran, P.O. Box 19575-361, Tehran, Iran*
[b] *Department of Biology, Faculty of Basic Science, Shahed University, Tehran, Iran*

Available online 20 December 2005

Abstract

Conventional lead-acid batteries are relatively heavy and thus have a low specific energy. Therefore, to improve the energy density, a lighter grid has been proposed. In this work, a novel lead-acid battery with high specific surface area negative foam current collectors was designed and constructed. The collectors were studied by cyclic voltametery (CV) and electrochemical impedance spectroscopy (EIS). The foam collectors were designed and suitable paste composition and formation algorithm was obtained. The basic cells were manufactured and its performance was evaluated. The results showed that the foam grids resistance was lower than that for lead grids and the specific surface area of the foam grids was very greater than lead grids. The foam battery has good discharge characteristics compared with common lead-acid batteries. The discharge curve was flat and negative mass utilization efficiency was higher than 50% when the cell was discharged with C5/5 A (137 Ah kg^{-1} negative active materials). The foam grids were used as negative electrode for various types of lead-acid batteries such as 60 Ah starter battery, 2, 3 and 10 Ah VRLA batteries. The batteries with foam grids were shown longer cycle life than conventional lead-acid batteries.

Keywords: Lead-acid battery; Negative electrode; Grid; Foam grid

1. Introduction

The lead-acid battery always has been the most important rechargeable electrochemical storage system, maintaining its prime position unchallenged now for more than a century. Conventional lead-acid batteries are relatively heavy and thus have a low specific energy [1]. The heavy weight of the battery is a direct result of the use of large amounts of lead in the plates, both in the grid and in the active material. Therefore, to improve the energy density, a systems approach to battery research and development involving all components, such as current collector structure [2–5], paste composition [6,7], charging protocol and charger design [8,9], thermal and electrolyte [10,11] management and overall battery is required. One way to achieve a higher energy density lead-acid battery is proposed, a grid with lighter weight and higher surface area than conventional grid. The lead grid in a lead-acid battery has two functions: as a current collector and as an active material supporter.

The utilization efficiency of the active mass and the cycle life of the lead-acid battery are determined by the complex phenomena occurring at the current collector–active material–electrolyte interface. It has been recognized that the design of the current collector structure, by its influence on the α (collector weight/plate weight) and γ (plate weight/collector surface area) factors characterizing the battery plates, has an important role with regard to active mass utilization and cycle life [12].

The objective of the work reported here is to develop valve-regulated lead-acid batteries (VRLA) and starter-lighting-ignition batteries (SLI) with foam grid that optimized for high specific energy and good cycle life. This objective is pursued by the extension of present technology to progressively higher plate utilization. Increase in plate utilization is attempted by reducing the grid mass and increasing the grid surface area.

2. Experimental

2.1. Instrumentation

Electrochemical experiment such as cyclic voltammetry and electrochemical impedance spectroscopy were performed using

* Corresponding author.
E-mail address: rahmanf_m@yahoo.com (M.S. Rahmanifar).

0378-7753/$ – see front matter © 2005 Elsevier B.V. All rights reserved.
doi:10.1016/j.jpowsour.2005.11.017

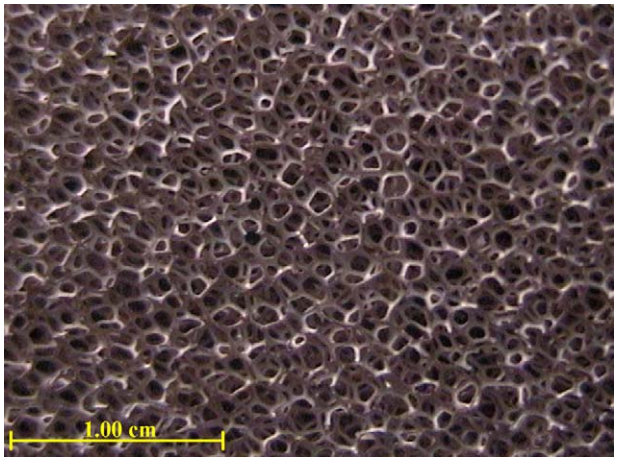

Fig. 1. Photograph of foam grid electroplated with Cu.

an Autolab PGS 100 high power potentiostat connected to a PIII PC and GPES ver. 4.9 software. Battery testing was performed using solartron 1247 BTS and cell test ver. 4.1.0 battery test system software.

2.2. Materials and reagents

The electrochemical experiments were carried out with a three-electrode arrangement. Lead foams with a geometric area 6.20 cm^2 were used as working electrode for electrochemical test. The thickness of the lead foam was 0.50 cm. The counter electrode was a plate Pt meshes with a geometric area 25.00 cm^2. A graph of a sponge-like porous metal matrix having spherical cells 1–2 mm in diameter and defined by grating is shown in Fig. 1.

2.3. Procedure

A grid material was formed of a three-dimensional reticulated sheet made of an organic foam compound. Electric conductivity can be given to the foam grid by using the electroless method [13] and then conductive foam grid was galvanostatically plated with a pure lead using a fluoroborate bath. For battery testing, 2 V single cell units were assembled using two positive 3 Ah conventional plates and one negative foam collectors. The current collectors were manually pasted using a PbO–$PbSO_4$ based paste from an industrial source. The entire foam plates was enclosed by an inverted glass beaker and placed inside an oven for applying the initial curing program. The following steps were used to initial curing program for:

Step 1: Foam plates were cured at 65–70 °C for 36 h at a relative humidity of 90%.
Step 2: Then 65–70 °C for 12 h at a relative humidity of 30%.

Fig. 2 shows a typical pasted collector design foam with a size of 7.00 cm × 4.50 cm × 0.50 cm (height × width × thickness).

The new thick foam grids need a suitable formation algorithm, but for primary test an initial formation algorithm was

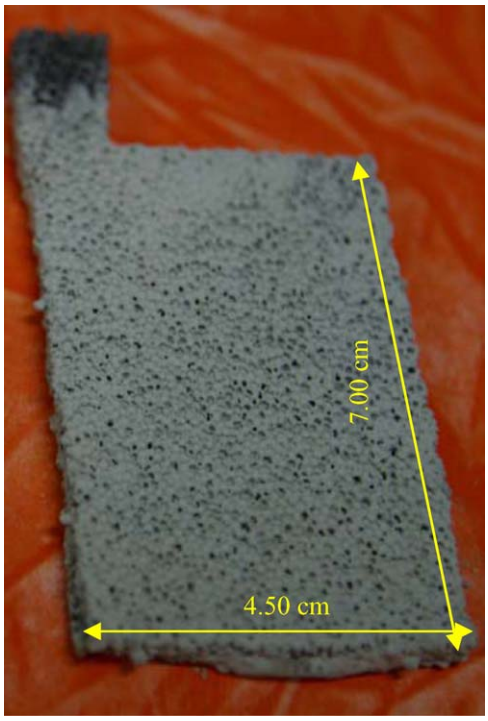

Fig. 2. Photograph of foam negative plate after curing.

performed in 1.05 g cm^{-3} H_2SO_4 (with seven charging steps) contain:

1. 1.0 h rate 2.5 mA g^{-1}.
2. 1.0 h rate 5.0 mA g^{-1}.
3. 1.0 h rate 7.5 mA g^{-1}.
4. 1.0 h rate 10.0 mA g^{-1}.
5. 1.0 h rate 12.5 mA g^{-1}.
6. 1.0 h rate 5.0 mA g^{-1}.
7. 0.5 h rest.

The formation was completed with repeating the steps 6 and 7.

For cell cycling experiments, the electrolyte was H_2SO_4 with an initial relative density of 1.30 at 298 °K. The discharge cut off voltage was 1.5 V.

3. Results and discussions

3.1. Electrochemical studies

The cyclic voltammograms of the Pb plate with 1.0, 1.9, 2.6, 4.0 cm^2 surface area and Pb electrodeposited foam grid in 5 M H_2SO_4 at 5 mV s^{-1} was recorded between −700 and 1300 mV (shown in Fig. 3). The Pb electrodeposited foam grid voltammogram showed the characteristic electrochemical features of pure Pb with very high anodic and cathodic peak intensity compare to pure lead.

The Nyquist plots of lead deposited foam grid in 5 M H_2SO_4 solution at equilibrium potential and Pb plate with 1.0, 1.9, 4.0 cm^2 surface areas is shown in Fig. 4. These figures indicate a charge transfer resistance and a mass transport component in

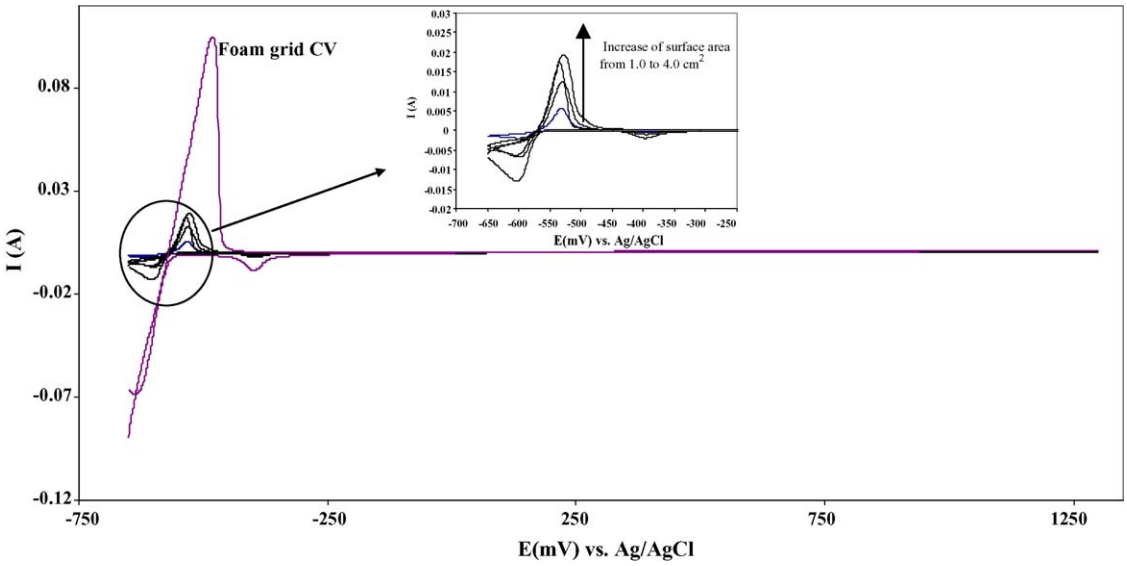

Fig. 3. Cyclic voltammograms of Pb plate with 1.0, 1.9, 2.6, 4.0 cm^2 surface area and Pb electrodeposited foam grid in 5 M H_2SO_4 at 5 mV s^{-1}.

parallel with a double layer capacitance. The increasing capacitance of foam grid in comparison with the capacitance of lead plates indicated that the active surface area of foam grid was higher than that lead grids.

3.2. Optimization of negative plate composition

The initial discharge test of metal foam showed a higher internal resistance and lower capacity than conventional casting Pb grids. So, to reduce initial resistance and increase the plate capacity two different types of carbon allotropes were used as additive for negative thick foam grids. The contents of acetylene black, as porous additive, and graphite, as conductive additive, in negative paste were studied between 0.2 and 10% (w/w).

3.2.1. Effect of acetylene black (AB) loading

Acetylene black, a porous additive, helps to absorption of electrolyte onto negative active material. The capacity density (CD) of negative foam plate depends on the amount of AB content. The variations of the CD of the negative paste as a function of CD of negative paste are given in Fig. 5. As is seen, CD of the negative paste increases with increasing content of AB in negative paste of cell with foam grid and reaches a maximum value for an AB loading of 1% (w/w). So, the optimum value was found around 1% weight of AB.

3.2.2. Effect of graphite loading

Graphite is added to the expander to improve the conductivity of the active material during deep discharges where the

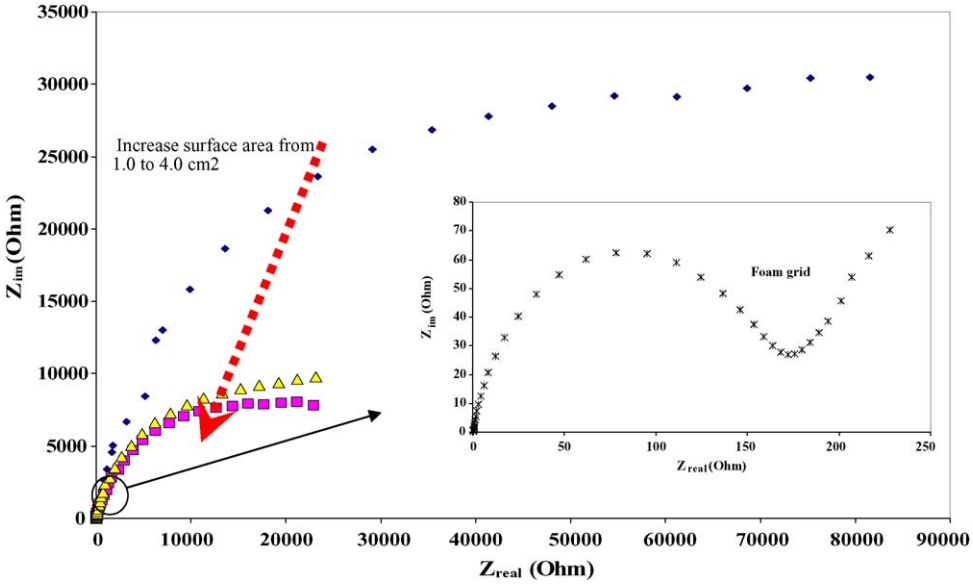

Fig. 4. Nyquist plot of Pb plate with 1.0, 1.9, 4.0 cm^2 surface area and Pb electrodeposited foam grid in 5 M H_2SO_4 at equilibrium potential.

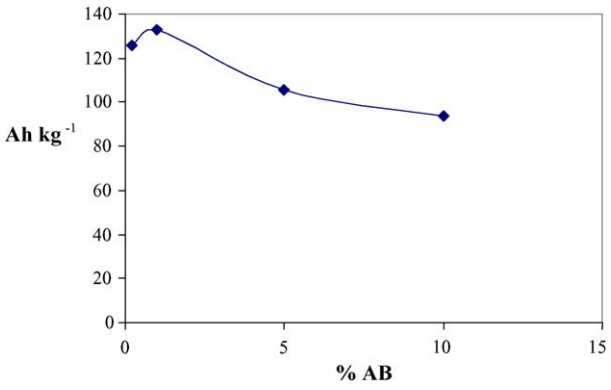

Fig. 5. Effect of acetylene black on negative paste capacity density of foam lead-acid battery.

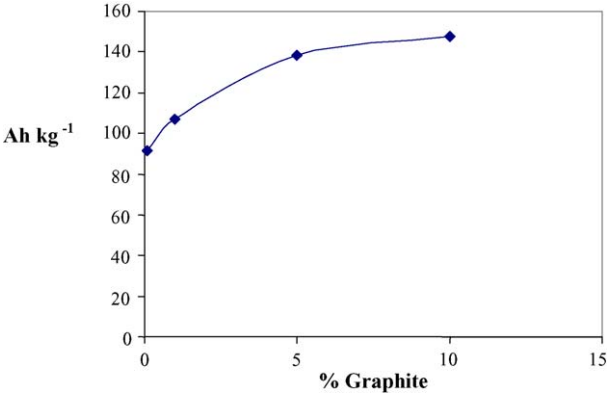

Fig. 6. Effect of graphite on negative paste capacity density of foam lead-acid battery.

concentration of highly resistant lead sulfate is high. Fig. 6 shows the effect of graphite content on the CD of negative paste. It is clearly observed that the CD of the negative paste increases with increasing the graphite loading of the negative paste. Because of the negative paste shedding after 1% (w/w), during charge discharge cycles, the 1% value was selected as the optimum amount of the graphite.

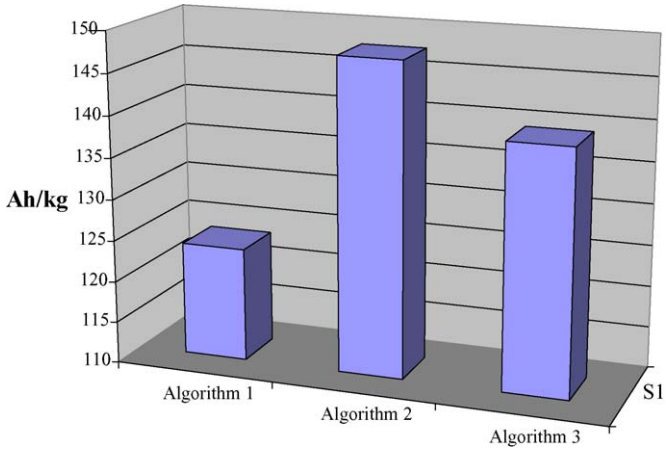

Fig. 7. Effect of formation algorithm on negative paste capacity density of foam lead-acid battery.

3.3. Development of a suitable formation algorithm

The battery manufacturer will need some experimentation to determine the most effective formation algorithm for a specific product. Formation, one of the final steps in battery production, is carried out by applying a charge to the cured plates immersed in sulfuric acid solution. During the formation process lead oxides are converted to sponge lead and lead dioxide on negative and positive electrode, respectively, by means of electrochemical reactions. The following algorithm can be used to selection of a suitable process.

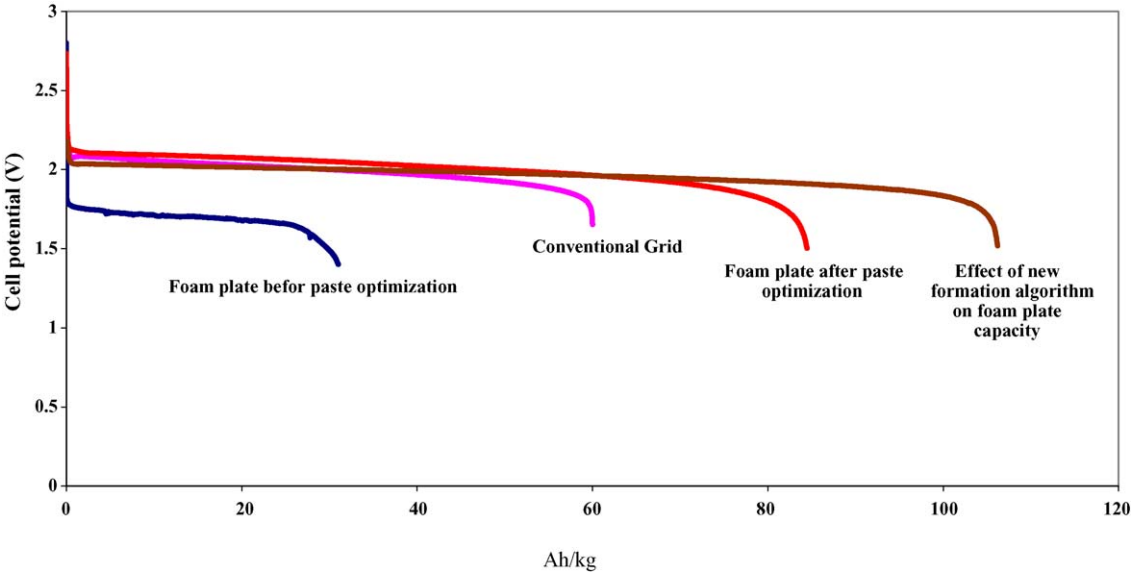

Fig. 8. Potential/capacity density of new type of lead-acid cell in comparing with conventional lead-acid cell.

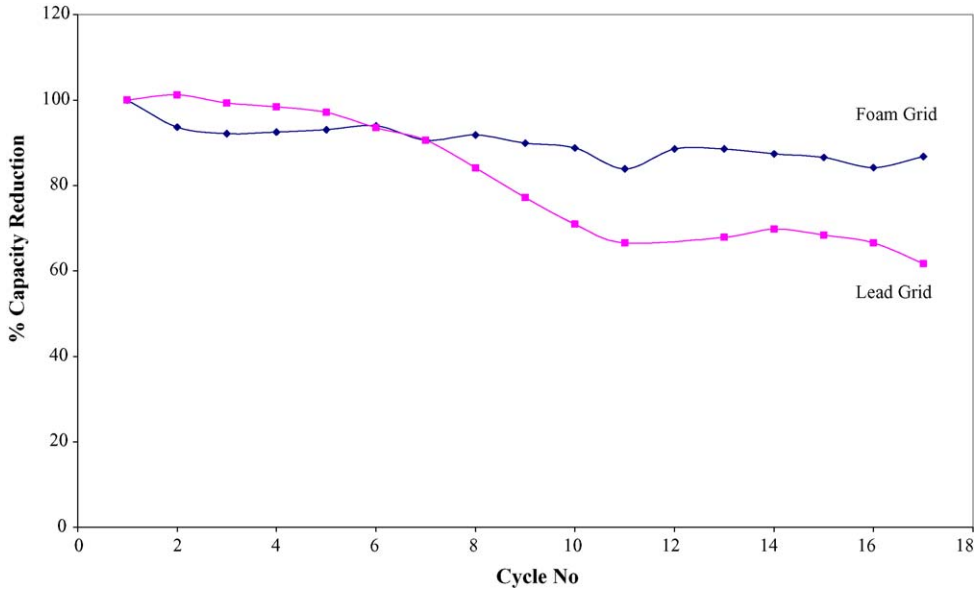

Fig. 9. Capacity reduction of cell with foam grid and lead grid (for deep discharge).

Algorithm 1	Same as initial algorithm
Algorithm 2	Step (1) 2.0 h rate 6.0 mA g^{-1} 3.0 h rate 12.0 mA g^{-1} 4.0 h rate 4.5 mA g^{-1} Step (2) 2.0 h rate 16.5 mA g^{-1} 0.5 h rest Step (3) 2.0 h rate 13.5 mA g^{-1} 0.5 h rest Step (4) 2.0 h rate 9.0 mA g^{-1} 0.5 h rest

The steps 2 and 3 of above algorithm were two and three times replication. The formation was completed with repeating the step 4.

Algorithm 3	1.0 h rate 3.2 mA g^{-1} 2.0 h rate 19.0 mA g^{-1} 4.0 h rate 12.7 mA g^{-1} 3.0 h rate 6.4 mA g^{-1} 0.5 h rest 3.0 h rate 4.8 mA g^{-1} 0.5 h rest

The formation was completed with repeating the steps 4–7.

The results revealed that, however, the initial capacity of plates that formed under algorithm no. 2 had the more capacity, but capacity reduction of algorithms nos. 1 and 2 was less than no. 3. Fig. 7 compares the capacity density of three formation algorithms.

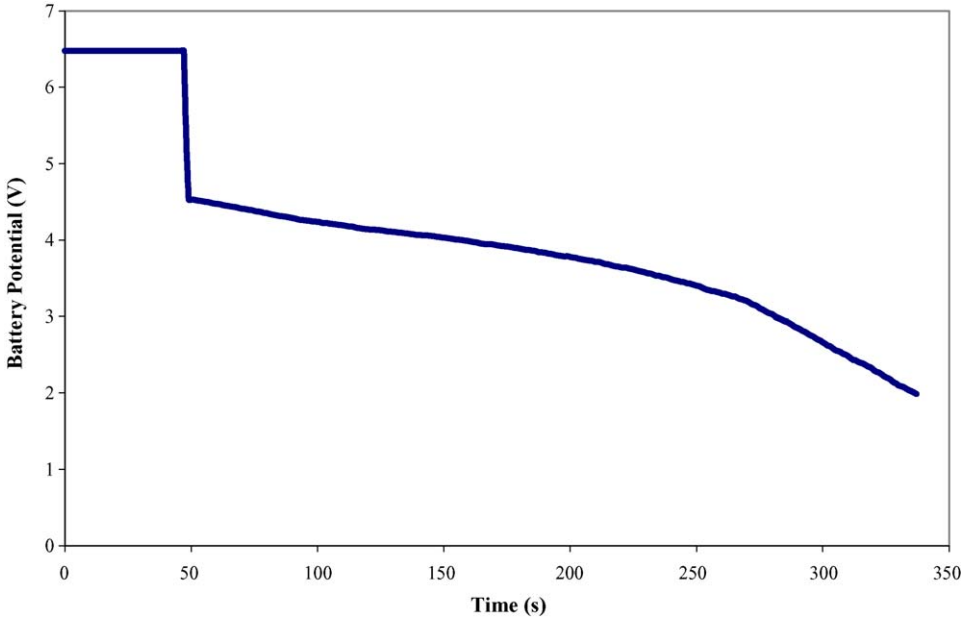

Fig. 10. Discharge of 60 Ah 6 V Foam battery with 200 A current.

3.4. Discharge experiments

The cells with negative foam grids were discharged with C5/5 A current and compare with conventional lead grids. Fig. 9 shows a typical potential/capacity density of lead-acid cell with foam grid before and after paste optimization that were compared with conventional lead grid. The discharge curve of cell with foam grid before paste optimization showed lower capacity density and higher cell resistance than cell with conventional lead grid. But after optimisation, both parameter had the better condition. In addition, because of the reducing of the cell resistance on cell with foam grid the power density was increased by 42% on the cell with foam grid. Furthermore, Fig. 8 indicates the capacity density of negative foam plate after applying the suitable curing program and formation algorithm. The foam plate's capacity density was increased by two-orders compare than the cast grids. The active material utilization was calculated for both foam and gravity cast grid. Results showed that the plates prepared with foam grids give higher active material utilization.

3.5. Cycle life

Fig. 9 shows the percentage of discharge capacity reduction against cycle number for the cells using foam grids and conventional cast grids. The cell with foam grids show lower capacity fall than cast grids.

4. Battery making

After cycle life test some various types of battery such as 60 Ah Starter battery, 2, 3 and 10 Ah sealed battery with foam grid were made and the standard tests such as DIN and JIS were done. The sealed batteries separators were AGM and for starter batteries were PVC. The sealed batteries filled with 1.30 g cm^{-3} H_2SO_4 and starter batteries with 1.28 g cm^{-3}.

A typical voltage–time curve during the discharging with 200 A current is shown in Fig. 10. This figure indicated that foam grid can be used as a suitable current collector for high rate discharge conditions.

5. Conclusion

New materials and process techniques have been defined in order to substitute the heavy lead grids used nowadays in commercial lead-acid batteries by the polymeric structure with a high conductivity due to the copper content and the higher active material utilization due to the optimized three-dimensional electrode structure and paste. The forecast applications are: SLI and VRLA batteries. The work on this subject is continuing.

Acknowledgment

The authors would like to acknowledge the Niru Battery Manufacturing Co. for their supports.

References

[1] http://www.kfb.se/ehvproge/r-00-53.pdf.
[2] E. Gyenge, J. Jungi, S. Splinter, A. Snaper, J. Appl. Electrochem. 32 (2002) 287.
[3] J. Wang, Z.P. Guo, S. Zhong, H.K. Liu, S.X. Dou, J. Appl. Electrochem. 33 (2003) 1057.
[4] A. Czerwinski, M. Zelazowska, J. Power Sources 64 (1997) 29.
[5] M.L. Soria, J. Fullea, F. Saez, F. Trinidad, J. Power Sources 78 (1999) 220.
[6] E. Bashtavelova, A. Winsel, J. Power Sources 53 (1995) 175.
[7] W.R. Kitchens, R.C. Osten, D.W.H. Lambert, J. Power Sources 53 (1995) 263.
[8] R.F. Nelson, E.D. Sexton, J.B. Olson, M. Keyser, A. Pesaran, J. Power Sources 88 (2000) 44.
[9] D. Calasanzio, M. Caselli, D. Ghiotto, J. Power Sources 53 (1995) 143.
[10] L. Torcheux, P. Lailler, J. Power Sources 95 (2001) 248.
[11] B. Monahov, D. Pavlov, A. Kirchev, S. Vasilev, J. Power Sources 113 (2003) 281.
[12] D. Pavlov, J. Power Sources 53 (1995) 9.
[13] Ullmann's Encyclopedia of Industrial Chemistry, sixth ed., vol. 11, p. 559.